# THE BEHAVIOR OF DOUBLE-LAP SPLICE BOLTED STEEL CONNECTIONS WITH FIBER-REINFORCED POLYMER FILLS

Kara D. Peterman
Northeastern University, Boston, Massachusetts 02115, USA
k.peterman@neu.edu

Julieta Moradei
Northeastern University, Boston, Massachusetts 02115, USA
moradei.j@husky.neu.edu

James D'Aloisio
Klepper Hahn and Hyatt, East Syracuse, New York 13057, USA
jad@khhpc.com

Mark Webster
Simpson Gumpertz and Heger, Waltham, Massachusetts 02453, USA
mdwebster@sgh.com

Jerome F. Hajjar
Northeastern University, Boston, Massachusetts 02115, USA
jf.hajjar@neu.edu

As researchers and practitioners look towards building sustainability, thermal bridges in steel structures become increasingly relevant. In order to mitigate these thermal bridges, structural thermal breaks are necessary to decrease energy loss at the building envelope. Options for improving the thermal insulation in steel buildings include exploring thermally improved materials such as fiber-reinforced polymers (FRP) and stainless steel, along with possible mitigation strategies fabricated from them to provide an effective thermal break without compromising structural integrity. Three-dimensional thermal modeling demonstrates the efficacy of these materials as thermal shims in shelf angles, roof posts, and canopy beams. However, non-steel fills in steel bolted connections are not clearly approved for use in steel structures, and currently, no methodology or test results exist to provide recommendations for their design and implementation. To validate the structural performance of these polymers in steel bolted connections, an array of experiments are conducted to explore these mitigation strategies. Several parameters are experimentally examined in the tests, including: bolt diameter, fill material, fill thickness, and the effect of multiple plies. This work, part of a larger ongoing research effort, aims to determine the behavior of these connections, and establish recommendations for their design and future use.

## INTRODUCTION

This study of thermal break strategies for cladding systems in steel structures aims to propose effective structural thermal breaks and validate them through extensive modeling and experimental testing. Thermal bridge mitigation strategies examined in this work range from inserting a thermally-improved shim into the bolted structural connections to replacing the structural member entirely with a thermally-improved member. Two materials explored to date include the use of fiber reinforced polymers (FRPs) and stainless steel. As FRPs differ in mechanical properties to steel, it is necessary to validate the behavior for these FRP fills in bolted steel connections, and under prolonged loading.

The use of steel fills in bolted steel connections has been previously explored by a number of researchers, e.g., Lee and Fisher (1968), Frank and Yura (1981), Dusicka and Lewis (2010), Borello et al. (2009, 2011), and Denavit et al. (2011). This research established that the strength of bolted connections in bearing may be reduced by up to 15%, with the reduction being a function of the thickness of the steel fills (AISC 2005, 2010).

There is limited research on the performance of FRP materials in steel structures, especially subjected to creep. Sa et al. (2011) summarizes previous work in creep experimental studies, which is limited to tension and compression in the plane of the fiber, and bending. However, no studies exist on FRP creep compression performance perpendicular to the plane of the fiber, the typical direction and mode of loading for fills in bolted steel connections.

The work presented here summarizes initial findings on the structural performance of FRP fills in bolted steel connections via thermal modeling, creep testing of FRP materials in compression perpendicular to the fibers, connection testing to establish bolt strength in the presence of shims, and sub-system testing of shelf angle connections. This ongoing research is also exploring the structural and thermal performance of roof posts and canopy beams with a variety of thermal break mitigation strategies.

## THERMAL MODELING

Thermal modeling of shelf angles and potential mitigation strategies was completed using the HEAT3 v7.0 software for three-dimensional configurations to demonstrate the efficacy of the thermal break strategies. Steady state thermal analysis was conducted to calculate the effective field of wall U-factor. The results for thermally-improved shims within the shelf angle connections are summarized below.

For the purpose of thermal modeling, all connections are designed to simulate the constructible cladding assemblies, in contrast to the structural test specimens, which are overdesigned in key components to assure that the primary failure mode of the cladding assembly will not be due to yielding at the connections (this is discussed below). For thermal modeling in HEAT3, surface areas of all materials must be in contact to transmit thermal energy. For example, all hole diameters are modeled with the same diameters as the rods for surface contact between the plates and the rods. Typical thermal gradients of unmitigated and mitigated models are shown in Figure 1.

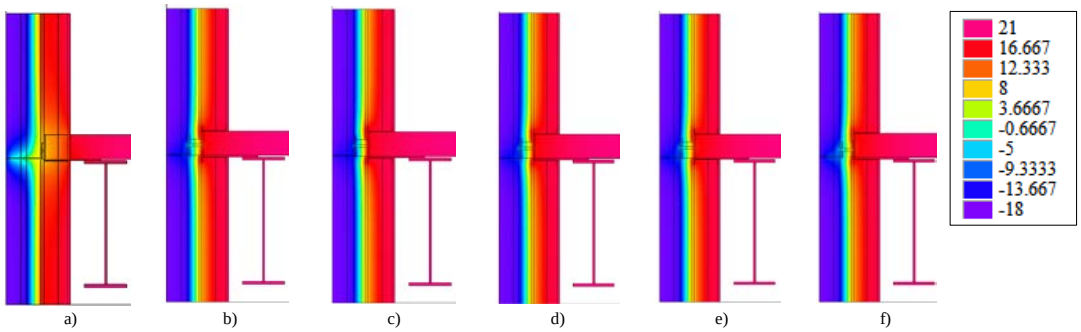


Figure 1: Thermal gradients of a) Unmitigated, b) Vinylester shim with A325 bolts (ΔU-value=50.22%), c) Vinylester shim with A304-SH bolts (ΔU-value=53.16%), d) Proprietary 1 shim (ΔU-value=54.32%), e) Proprietary 2 shim (ΔU-value=54.05%), f) Stainless tube shim (ΔU-value=47.73%) – units in degrees Celcius.

The interior and exterior boundary conditions are based on prescribed values in Normative Appendix A of ASHRAE 90.1-2013 and NFRC 100-2014. An interior ambient temperature of 69.8°F and an exterior ambient temperature of –0.4°F were assumed in accordance with NFRC-2014. These results show that mitigation via thermally improved shims (and by extension, intermittent spacing of the angle along the length due to shimming) improves the thermal conductivity of the system by 47-54%, depending on material. Typical results are tabulated in Table 1 below.

Table 1: Selected thermal modeling results from shelf angle modeling efforts

| Unmitiagated Model | | | Mitigated Model | | | | Comparison | |
|---|---|---|---|---|---|---|---|---|
| Model Name (-) | Bolt Type (-) | U-Value (BTU/h*ft2*°F) | Model Name (-) | Shim Material (-) | Bolt Type (-) | U-Value (BTU/h*ft2*°F) | Δ U-Value (BTU/h*ft2*°F) | %-Reduction |
| Shelf Angle Unmitigated 2.5 Inch_S1_V2 | A304-SH | 0.138 | Shelf Angle Mitigated 2.5 Inch_S8_V3 | Vinylester shim | A325 | 0.082 | 0.056 | 40.41 |
| Shelf Angle Unmitigated 2.5 Inch_S1_V2 | A304-SH | 0.138 | Shelf Angle FRP 2.5 Inch_S19 | FRP angle | A304-SH | 0.072 | 0.066 | 47.94 |
| Shelf Angle Unmitigated 5 Inch_S4_V2 | A304-SH | 0.112 | Shelf Angle Mitigated 5 Inch_S14.1_V3 | Vinylester shim | A325 | 0.056 | 0.056 | 50.22 |
| Shelf Angle Unmitigated 5 Inch_S4_V2 | A304-SH | 0.112 | Shelf Angle Mitigated 5 Inch_S14.2_V3 | Vinylester shim | A304-SH | 0.053 | 0.060 | 53.16 |
| Shelf Angle Unmitigated 5 Inch_S4_V2 | A304-SH | 0.112 | Shelf Angle Mitigated 5 Inch_S17_V3 | Proprietary 1 shim | A304-SH | 0.051 | 0.061 | 54.32 |
| Shelf Angle Unmitigated 5 Inch_S4_V2 | A304-SH | 0.112 | Shelf Angle Mitigated 5 Inch_S18.1_V3 | Proprietary 2 shim | A304-SH | 0.052 | 0.061 | 54.05 |
| Shelf Angle Unmitigated 5 Inch_S4_V2 | A304-SH | 0.112 | Shelf Angle Mitigated 5 Inch_S18.2_V3 | Stainless tube shim | A304-SH | 0.059 | 0.054 | 47.73 |

## CONNECTION TESTING PROGRAM

Double lap splice bolted connections were considered in this experimental program, analogous to the configurations for steel fills in Lee and Fisher (1968), Frank and Yura

(1981), Dusicka and Lewis (2010), Borello et al. (2009, 2011), and Denavit et al. (2011). The test rig is shown in Figure 2. The base of the connection was designed to be essentially rigid and is fixed in the test rig, a 600 kip Forney universal testing machine located at the Simpson Gumpertz and Heger laboratory in Waltham, MA. Monotonic load is applied to the top of the connection at a rate of 1 kip/second. Two bolts were used to decrease variation in the connection strength.

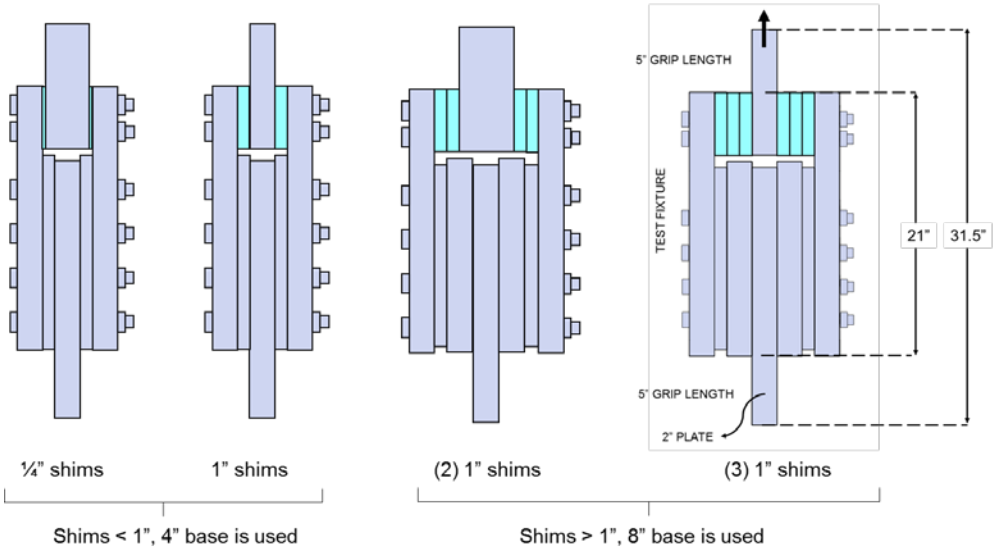


Figure 2: Connection test setup illustrating various shim thickness configurations

The rig base is fixed in the test rig and was designed not to fail. Similarly, the side plates on the outside of the text fixture as well as the interior top plate were designed to force failure into the bolts. To ensure that the interior top plate does not fail, two base fixtures (4 inch base and 8 inch base) were designed so that thicker shims may be tested without compromising strength of the fixture. The interior top plate and side plates are replaced after each test, while the base plates are reused.

The test matrix for the experimental program is shown in Table 2. Bolt material as well as diameter are varied. As stainless steel is less thermally conductive that carbon steel, A304-SH bolts (strain-hardened stainless steel bolts matching closely in strength properties to A325 carbon bolts) were included in the study. FRP shim thickness is also varied from ¼ inch to 3 inches. Multiple FRP plies are not bonded together (note: 1" shims were delivered as two ½" shims bonded together).

Testing is in progress, but a comparison between the tested specimens (3" thick vinylester shims and no shims, each with two 5/8" dia. A325 bolts) in Figure 3 demonstrates that peak strength decreases by 37% and stiffness decreases by a factor of 6.5.

The vinylester shims in test C16 ovalized significantly, and delaminated at the bond line at the midpoint of the cross section. This behavior contributed to the overall ductility of the system when compared to test C1 without shims.

Table 2: Connection test matrix (completed tests are shaded)

| | | | | | | Rig Thicknesses | |
|---|---|---|---|---|---|---|---|
| **Test Name** | **Shim Type** | **Shim Thickness** | **Bolt Dia. (in)** | **Bolt Spec** | **Hole Size*** | **Top** | **Bottom** |
| C1 | no shim | - | 5/8 | A325 | 11/16 | 4" | 4" |
| C2 | no shim | - | 5/8 | A304 SH1 | 11/16 | 4" | 4" |
| C3 | no shim | - | 1/2 | A325 | 9/16 | 4" | 4" |
| C4 | polyurethane | 1/4" | 5/8 | A325 | 11/16 | 3.5" | 4" |
| C5 | vinylester | 1/4" | 5/8 | A325 | 11/16 | 3.5" | 4" |
| C6 | phenolic | 1/4" | 5/8 | A325 | 11/16 | 3.5" | 4" |
| C7 | proprietary 1 | 1/4" | 5/8 | A325 | 11/16 | 3.5" | 4" |
| C8 | proprietary 2 | 1/4" | 5/8 | A325 | 11/16 | 3.5" | 4" |
| C9 | vinylester | 2x1/2" multiple plies | 5/8 | A325 | 11/16 | 2" | 4" |
| C10 | vinylester | 1" | 5/8 | A325 | 11/16 | 2" | 4" |
| C11 | vinylester | 1" | 5/8 | A304 SH1 | 11/16 | 2" | 4" |
| C12 | vinylester | 1" | 1/2 | A325 | 9/16 | 2" | 4" |
| C13 | vinylester | 2x1" multiple plies | 5/8 | A325 | 11/16 | 4" | 8" |
| C14 | vinylester | 2x1" multiple plies | 5/8 | A304 SH1 | 11/16 | 4" | 8" |
| C15 | vinylester | 2x1" multiple plies | 1/2 | A325 | 9/16 | 4" | 8" |
| C16 | vinylester | 3x1" multiple plies | 5/8 | A325 | 11/16 | 2" | 8" |
| C17 | vinylester | 3x1" multiple plies | 5/8 | A304 SH1 | 11/16 | 2" | 8" |
| C18 | vinylester | 3x1" multiple plies | 1/2 | A325 | 9/16 | 2" | 8" |

*holes are standard holes (bolt dia. + 1/16")

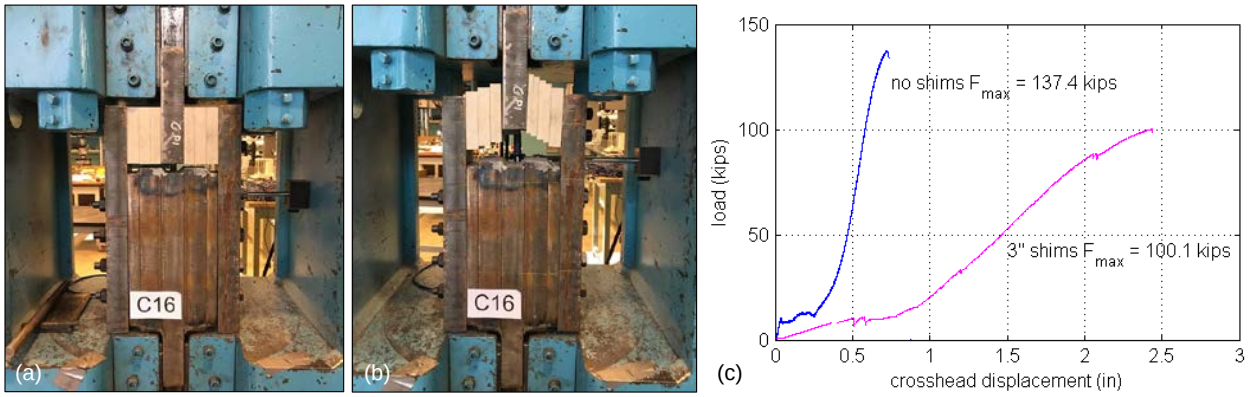


Figure 3: (a) Test C16 (3" vinylester shims, 5/8" dia. A325 bolts) pre-test (b) Test C16 post-test, depicting shim delamination and extent of deformation (c) comparison between no shims case (test C1) and test C16.

## MATERIAL CREEP TESTING PROGRAM

The long term behavior of FRP fills is validated via creep testing at the material level. As currently there exists no standard or precedent for creep testing of FRP materials in bearing compression, existing standards for creep testing in tension and compression were referenced to construct the following creep testing protocol. Testing is conducted in a 100 kip MTS testing machine, with load held constant over time and displacements measured over time. Failure typically occurs at approximately the same strain level regardless of the loading and time to failure, until the load is low enough that it is below a threshold such that failure due to creep is not anticipated. Stress ratios ($\sigma_{app}/\sigma_{max}$) are

determined based on the time to failure, $t_f$. A successful panel of tests consists of tests with $t_f$ in three different logarithmic decades ($10^0$, $10^1$, $10^2$, etc), as illustrated in Figure 4.

| material | specimen | $t_f$ (hr) |
|---|---|---|
| vinylester | 1 | 1 |
| | 2 | 10 |
| | 3 | 100 |
| | 4 | 1000 |
| polyurethane | 1 | 1 |
| | 2 | 10 |
| | 3 | 100 |
| | 4 | 1000 |
| phenolic | 1 | 1 |
| | 2 | 10 |
| | 3 | 100 |
| | 4 | 1000 |
| proprietary 1 | 1 | 1 |
| | 2 | 10 |
| | 3 | 100 |
| | 4 | 1000 |
| proprietary 2 | 1 | 1 |
| | 2 | 10 |
| | 3 | 100 |
| | 4 | 1000 |

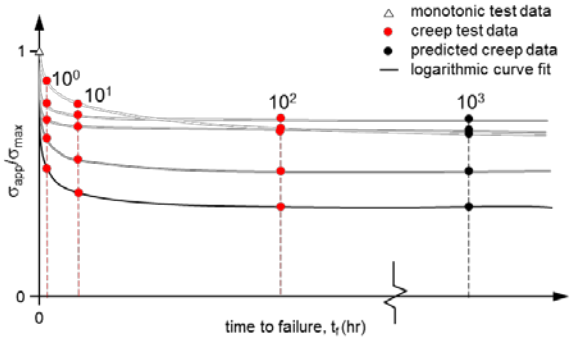


1. Perform creep tests such that $t_f$ varies by logarithmic decades
2. Fit logarithmic curve to experimental data
3. Predict ($t_f$ , $\sigma_{app}/\sigma_{max}$) for material performance beyond seven days

Figure 4: Ideal creep testing matrix and protocol

As each material behaves differently under prolonged loading, the stress ratios that result in failure in each logarithmic decade will differ between the materials tested. The resulting test matrix with time-to-failure results from this work is shown in Table 3 below.

Table 3: Creep results across material types

| | | | | $t_f$, time to failure (hr) | | | | |
|---|---|---|---|---|---|---|---|---|
| material | specimen | $\sigma_{app}/\sigma_{max}$ | $F_{app}$ (kip) | $<10^0$ | $>10^0$ | $>10^1$ | $>10^2$ | $>10^3$ |
| vinylester | 3c | 0.8 | 21.28 | 0.628 | - | - | - | - |
| | 1c | 0.8 | 20.98 | - | 2.79 | - | - | - |
| | 2c | 0.8 | 20.93 | - | 3.30 | - | - | - |
| | 5c | 0.758 | 20.78 | - | 6.23 | - | - | - |
| | 6c | 0.75 | 20.10 | - | - | 13.4 | - | - |
| | 4c | 0.7 | 19.11 | - | - | - | 132 | - |
| polyurethane | 1c | 0.9 | 54.68 | 0.127 | - | - | - | - |
| | 2c | 0.9 | 54.45 | 0.785 | - | - | - | - |
| | 3c | 0.9 | 54.01 | - | 6.09 | - | - | - |
| | 4c | 0.8 | 44.03 | - | - | 36.9 | - | - |
| | 5c | 0.78 | 43.46 | - | - | - | 500+ | - |
| phenolic | 8c | 0.875 | 12.85 | - | - | - | 125+ | - |
| | 3c | 0.85 | 12.31 | - | 1.92 | - | - | - |
| | 7c | 0.85 | 12.49 | - | 9.63 | - | - | - |
| | 5c | 0.84 | 12.58 | - | - | 73.0 | - | - |
| | 2c | 0.8 | 12.11 | - | - | - | 231 | - |
| proprietary 1 | 2c | 0.85 | 27.84 | - | 3.08 | - | - | - |
| | 1c | 0.8 | 28.15 | - | - | 16.7 | - | - |
| | 3c | 0.78 | 27.16 | - | - | - | 146 | - |
| proprietary 2 | 1c | 0.8 | 26.76 | 0.214 | - | - | - | - |
| | 2c | 0.7 | 22.49 | - | 2.27 | - | - | - |
| | 6c | 0.69 | 21.63 | - | 6.68 | - | - | - |
| | 5c | 0.65 | 21.13 | - | - | 85.4 | - | - |

*not tested to failure

Time to failure and stress ratio are plotted against each other in Figure 5, with an example logarithmic/power curve fit of the vinylester creep data provided in the inset plot.

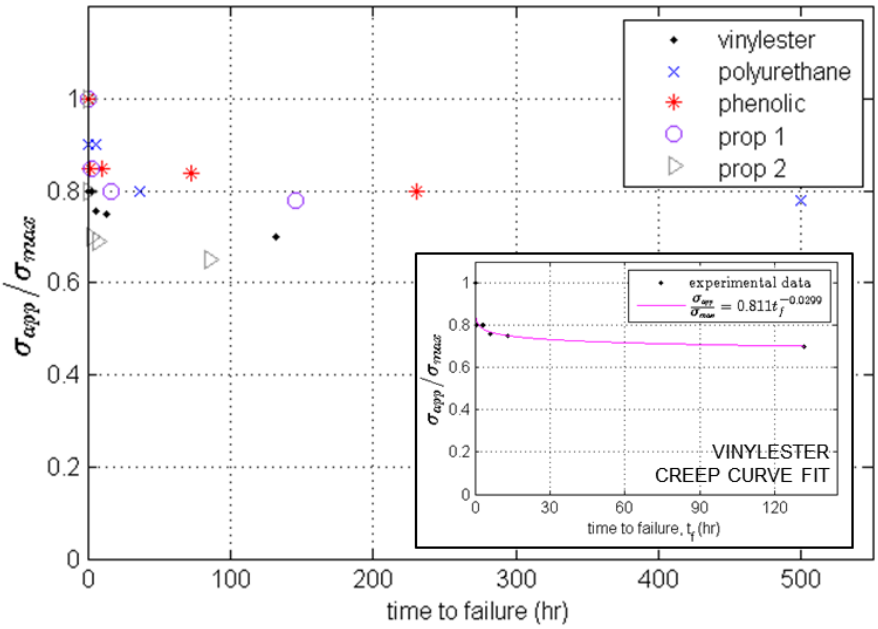


Figure 5: Creep time to failure versus applied stress ratio across tested materials. Inset, power curve fit of vinlyester experimental data.

Initial results indicate high variability in tests with high applied stress ratios (85-90% of ultimate stress). Additional repetitions at lower force ratios must be performed to completely characterize the variability of experimental results. Results also indicate an asymptote for each material at which the time to failure dramatically increases; this horizontal asymptote provides an upper boundary of the potential design space for these materials.

## SHELF ANGLE SUB-SYSTEM TESTING

To examine the performance of thick FRP shims in shelf angle cladding details, shelf angles with varying bolted connections and thermal break mitigation strategies were examined. As shelf angles are typically deflection-limited, connection strength is non-critical; 5/8” diameter bolts are commonly used. However, in order to observe experimental behavior beyond connection limits, specimens were designed as “designed” (with typical connections) and “over-designed” (with over-sized 1” diameter bolts). Shim material and thickness (corresponding to climate zone insulation specifications) were also varied. Shims were of constant area, 3x4” in size and centered on the shelf angle vertical flange, with the connection bolt passing through the center. The experimental test matrix is shown in Table 4.

Table 4: Shelf angle test matrix (completed tests are shaded)

| | | Mitigation Strategy | | | Specimen Information | | | |
|---|---|---|---|---|---|---|---|---|
| **Test Name** | **Specimen Type** | **Type** | **Material** | **Thick (in)** | **Length** | **Section** | **Bolt/Stud Spec** | **Bolt Dia. (in)*** |
| S1 | designed | - | - | - | 42 | L6x4x5/16 | A325 | 0.625 |
| S2 | designed | - | - | - | 42 | L6x4x5/16 | A304-SH | 0.75 |
| S3 | over-designed | - | - | - | 42 | L6x4x5/16 | A325 | 1 |
| S4 | designed | - | - | - | 42 | L7x4x3/8 | A325 | 0.625 |
| S5 | designed | - | - | - | 42 | L7x4x3/8 | A304-SH | 0.75 |
| S6 | over-designed | - | - | - | 42 | L7x4x3/8 | A325 | 1 |
| S7 | over-designed | shim | vinylester | 1.5 | 42 | L6x4x5/16 | A325 | 1 |
| S8 | designed | shim | vinylester | 1.5 | 42 | L6x4x5/16 | A325 | 0.625 |
| S9 | over-designed | shim | polyurethane | 1.5 | 42 | L6x4x5/16 | A325 | 1 |
| S10 | over-designed | shim | phenolic | 1.5 | 42 | L6x4x5/16 | A325 | 1 |
| S11 | over-designed | shim | proprietary 1 | 1.5 | 42 | L6x4x5/16 | A325 | 1 |
| S12 | over-designed | shim | proprietary 2 | 1.5 | 42 | L6x4x5/16 | A325 | 1 |
| S13 | over-designed | shim | vinylester | 3 | 42 | L7x4x3/8 | A325 | 1 |
| S14 | designed | shim | vinylester | 3 | 42 | L7x4x3/8 | A325 | 0.625 |
| S15 | over-designed | shim | polyurethane | 3 | 42 | L7x4x3/8 | A325 | 1 |
| S16 | over-designed | shim | phenolic | 3 | 42 | L7x4x3/8 | A325 | 1 |
| S17 | over-designed | shim | proprietary 1 | 3 | 42 | L7x4x3/8 | A325 | 1 |
| S18 | over-designed | shim | proprietary 2 | 3 | 42 | L7x4x3/8 | A325 | 1 |
| S19 | over-designed | FRP angle | vinylester | - | 42 | FRP L6x4x1/2 | A325 | 1 |
| S20 | over-designed | tube shim | carbon steel | HSS3x3x3/8 | 42 | L7x4x3/8 | A325 | 1 |
| S21 | over-designed | steel shim | carbon steel | 3 | 42 | L7x4x3/8 | A325 | 1 |

*holes are standard holes (bolt diamter + 1/16 inch)

The test rig is depicted in Figure 6. A load beam, designed to simulate loading from brick veneer in a typical installed configuration, compresses the horizontal leg of the shelf angle at a monotonic rate of 0.002 inches/second. Angles are loaded equidistant from the slab plate, regardless of the presence of shims, to maintain wall cavity size between mitigated and unmitigated shelf angles.

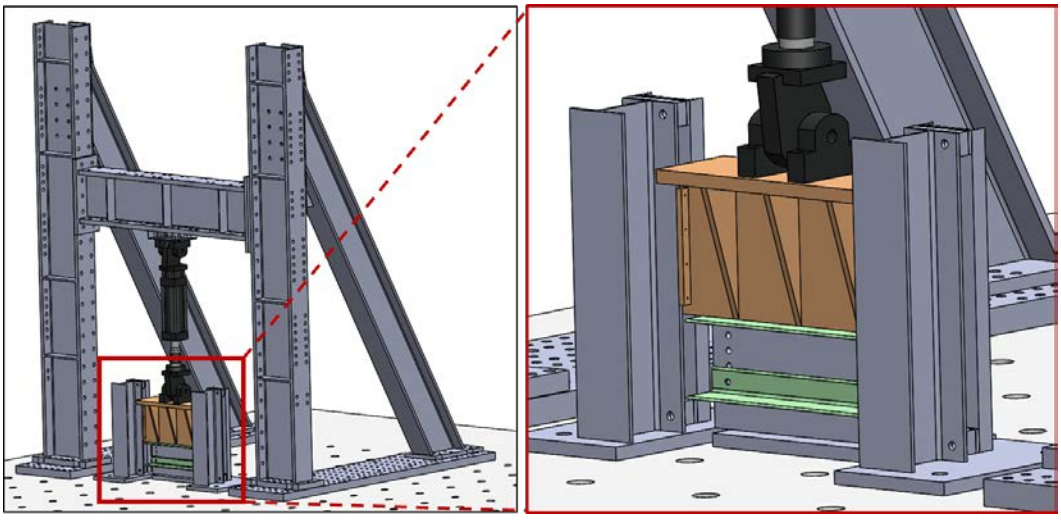

Figure 6: Shelf angle test rig with detail

A comparison of performance for specimens with 3” shims is presented in Figure 7. As the shimmed specimens are loaded nearer to the slab plate, these systems experience an increase in strength and stiffness from the unmitigated details.

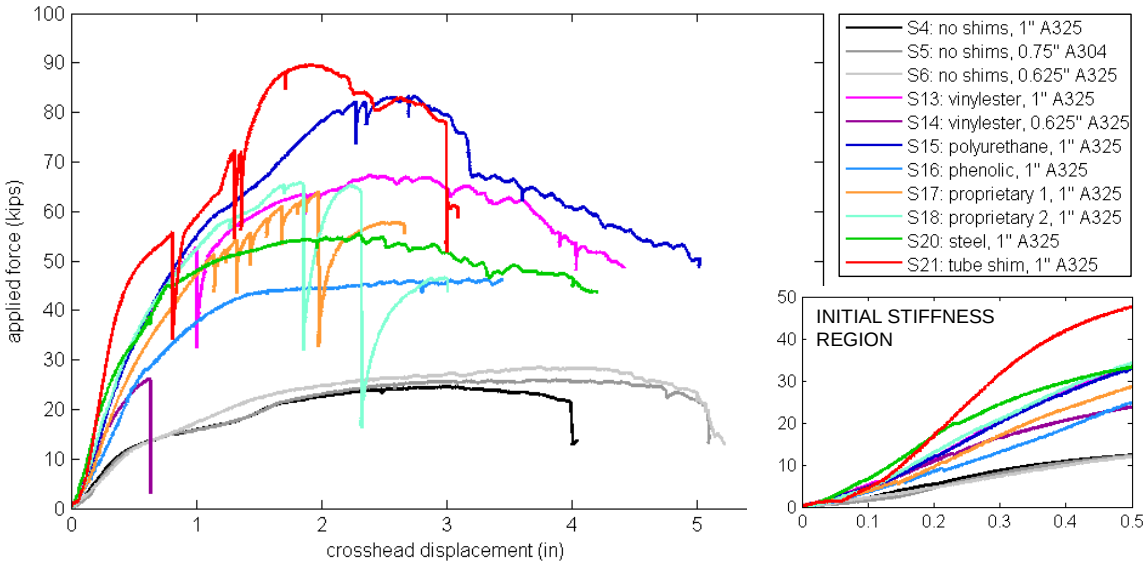


Figure 7: Force-displacement results for climate zone 7 shelf angles (L7x4x3/8) with shim thickness equivalent to required insulation layer (~3").

As Figure 7 illustrates, the unmitigated specimens perform similarly regardless of bolt diameter and material, notably so in the initial stiffness region. Steel shims (representing an intermittently spaced mitigation strategy) and tube shims result in the stiffest mitigated systems. One marked difference between the behavior of these two non-FRP mitigation strategies is that buckling of the tube shim ultimately permits additional deformation of the shelf angle, while the rigidity of the steel shims causes fracture of the shelf angle prematurely; this is borne out in a 38.5% reduction in peak strength of the steel shim specimen relative to the tube shim specimen. Similarly to the steel shims, the polyurethane shims did not fail during testing, resulting in fracture of the shelf angle at the heel. This failure mode is unique among the FRP shimmed specimens in that typically the shims crushed and delaminated while the angle deformed but did not fracture.

## CONCLUSIONS & FUTURE WORK

Connection, creep, and shelf angle testing all indicate potential for the use of FRP materials in bolted steel connections and sub-systems. Proposed solutions for thermal bridging in shelf angles demonstrate improved strength and stiffness from the unmitigated cases, in addition to reducing the thermal conductivity of the system between 40 and 50%. Performance of FRP materials under prolonged loads is promising; across the materials examined herein, creep does occur, but only in stress ranges well above typical design regions. Connection testing thus far demonstrates similarity with previous work in bolted steel connections with steel fills with respect to having a stiffness reduction between thick shimmed specimens and specimens without shims. The research summarized in this work is ongoing, with the aim of validating the use of FRP fills in steel bolted connections and in shelf angle cladding details through thermal modeling, sub-system testing, and creep testing, so as to provide design guidance for engineers. Additional tests are required to fully understand the behavior of FRP material under prolonged load. Shelf

angle, roof post, and canopy beam testing is currently in progress to explore the performance of connections with various moment-to-shear ratios and with various types of FRP and proprietary shims.

## ACKNOWLEDGEMENTS

This material is based upon work supported by the Charles Pankow Foundation, the American Institute of Steel Construction, the American Composites Manufacturers Association (ACMA), the ACMA-Pultrusion Industry Council, Schöck AG, the National Science Foundation under Grant No. CMMI-0654176, Simpson Gumpertz & Heger Inc., Klepper, Hahn & Hyatt, and Northeastern University. The authors would like to thank Kyle Coleman, Michael McNeil, Kurt Braun, Justin Kordas, Elisa Livingston, Madeline Augustine, and Dennis Rogers of Northeastern University, project team members Pedro Sifre, Mehdi Zarghamee, James Parker, Sean O'Brien, Jason Der Ananian, Nathalie Skaf, and Jessica Coolbaugh of Simpson Gumpertz & Heger and the members of the Industrial Advisory Panel and the ACMA Pultrusion Industry Council Technical Advisory Team. Any opinions, findings, and conclusions expressed in this material are those of the authors and do not necessarily reflect the views of the sponsors.

## REFERENCES

American Institute of Steel Construction (AISC) (2005). Specification for Structural Steel Buildings, ANSI/AISC 360–05, AISC, Chicago, Illinois.

American Institute of Steel Construction (AISC) (2010). Specification for Structural Steel Buildings, ANSI/AISC 360–10, AISC, Chicago, Illinois.

Borello D. J., Denavit, M. D., and Hajjar, J. F. (2009). "Behavior of Bolted Steel Slip-Critical Connections with Fillers," Report No. NSEL–017, Newmark Structural Laboratory Report Series, Department of Civil and Envirnomental Engineering, University of Illinois at Urbana-Champaign, Urbana, Illinois.

Borello D. J., Denavit, M. D., and Hajjar, J. F. (2011). "Bolted Steel Slip-Critical Connections with Fillers: I. Performance," *Journal of Constructional Steel Research*, Vol. 67, No. 3, pp. 379–88.

Denavit, M. D., Borello D. J., and Hajjar, J. F. (2011). "Bolted Steel Slip-Critical Connections with Fillers: II. Behavior," *Journal of Constructional Steel Research*, Vol. 67, No. 3, pp. 398–406.

Dusicka, P. and Lewis, G. (2010). High Strength Steel Bolted Connections with Filler Plate," *Journal of Constructional Steel Research*, Vol. 66, pp. 75–84.

Frank K. H. and Yura J. A. (1981). An Experimental Study of Bolted Shear Connections," Report No. FHWA/RD-81/148. Federal Highway Administration, U.S. Department of Transportation, Washington, DC, December.

Lee, J. H and Fisher, J. W. (1968). "Bolted Joints with Rectangular of Circular Fillers," Report No. 318.6., Fritz Engineering Laboratory, Department of Civil Engineering, Lehigh University, Bethlehem, Pennsylvania, June.

Sa, M. F., Gomes, A. M, Correia, J. R., and Silvestre, N. (2011). Creep Behavior of Pultruded GFRP Elements – Part I: Literature Review and Experimental Study," *Composite Structures,* Vol. 93, pp. 2450-2459.